Effects of specimen thickness and skeletal structure on consolidation behavior around consolidation yield stress

Effets de l'épaisseur du spécimen et de la structure du sol sur le comportement en consolidation autour de la pression de préconsolidation

Y. Watabe, M. Tanaka & S. Sassa
Port and Airport Research Institute, Yokosuka, Japan
M. Kobayashi
Coastal Development Institute of Technology, Tokyo, Japan
K. Udaka
Oyo Corporation, Saitama, Japan

ABSTRACT
The objective of this study is to empirically clarify the scale effect in long-term consolidation behavior. A series of inter-connected type consolidation tests was carried out. The strains for the clays with low viscosity effect followed the hypothesis A, in contrast, the strains for the clays with high viscosity effect followed the hypothesis B. The temporal variations of excess pore pressure for the clays with a highly developed structure are characterized by two staged dissipation curves.

RÉSUMÉ
L'objectif de cette étude est de clarifier empiriquement les effets de l'épaisseur de spécimen sur la consolidation à long-terme. Une série d'essais de consolidation inter-connectés a été effectuée. Les deformations pour les argiles avec un faible de effet viscosité suivent l'hypothèse A, mais, les deformations pour les argiles avec un fort effect de viscosité suivent l'hypothèse B. La variation temporelle de l'excès de pression interstitielle de l'argile avec une structure très développée se caractérise par deux étapes de dissipation.

Keywords: thickness effect, scale effect, inter-connected oedometer, structure, viscosity

1 INTRODUCTION

Generally, the consolidation test is conducted using a specimen with small dimensions, e.g., thickness of 20 mm. The test result is used to predict the in situ consolidation settlement of thick clay deposits. The consolidation test is a type of boundary-value problem. Therefore, the scale/thickness effect must be considered. Ladd et al. (1977) and Jamiolkowski et al. (1985) have pointed out and explained this relationship by using the two hypotheses shown in Fig.1.

In hypothesis A, the creep compression occurs only after the end of primary consolidation (EOP). Therefore, the law of squared H is applicable, resulting in the same value of the compressive strain at EOP in both the field and the laboratory. In contrast, in hypothesis B, the creep compression occurs even during the dissipation of excess pore water pressure and is governed by structural viscosity. Therefore, the law of squared H is not applicable, resulting in a large compressive strain with the thickness.

Aboshi (1973) reported that a relatively large scale consolidation test resulted in a behavior between the hypotheses A and B. The objective of this study is to empirically clarify the scale effect through a series of inter-connected type consolidation tests, in which each specimen element was individually loaded. Each specimen size was limited to a thickness of 20 mm such that the friction effect was minimized.

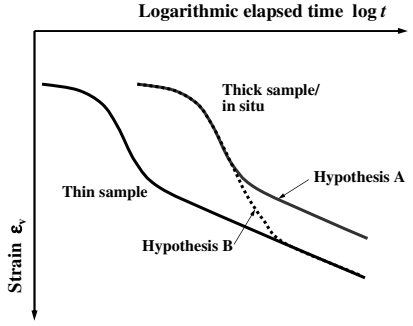

Fig. 1. Comparison between consolidation curves of a thin specimen and a thick specimen/in situ deposit.

2 INTER-CONNECTED TYPE CONSOLIDATION TEST

The tests were carried out for specimen thicknesses of 20 mm (H2), consisted of 2 elements with a thickness of 10 mm, and 100 mm (H10), consisted of 5 elements with a thickness of 20 mm, in the single drainage boundary condition. Even the case of 100-mm thickness is much thinner than the in situ condition; however, it is a realistic condition in the laboratory.

The soil samples examined were undisturbed Ma13 (Holocene) and Ma12 (Pleistocene) clays retrieved from the seabed of the Kansai International Airport, and Louiseville clay retrieved from the very sensitive clay deposits in eastern Canada. The physical and consolidation properties of the clay samples are listed in Table 1. Ma12 has a highly developed structure as can be expected from a high void ratio equivalent to Ma13. In addition, Louiseville clay is well known as sensitive clay with a highly overconsolidated stress history and developed structure. The specimen elements were trimmed and individually inserted into the consolidation rings with an inner diameter of 60 mm

Table 1. Physical and mechanical properties of soils.

Clay samples	Osaka Bay		Eastern Canada
	Ma13	Ma12	Louiseville
Overburden effective stress σ'_{v0} (kPa)	65	291	62
Consolidation yield stress p_c (kPa)	106	452	190
Overconsolidation ratio OCR	1.63	1.55	3.06
Soil particle density ρ_s (g/cm^3)	2.67	2.67	2.75
Liquid limit w_L	91.2	104.6	78.7
Plastic limit w_p	37.2	40.5	21.6
Plasticity index I_p	54.0	64.1	57.1
Natural water content w_n	83.3	82.2	68.3
Natural void ratio e_0	2.22	2.20	1.88

Proceedings of the 17th International Conference on Soil Mechanics and Geotechnical Engineering
M. Hamza et al. (Eds.)

doi:10.3233/978-1-60750-031-5-696

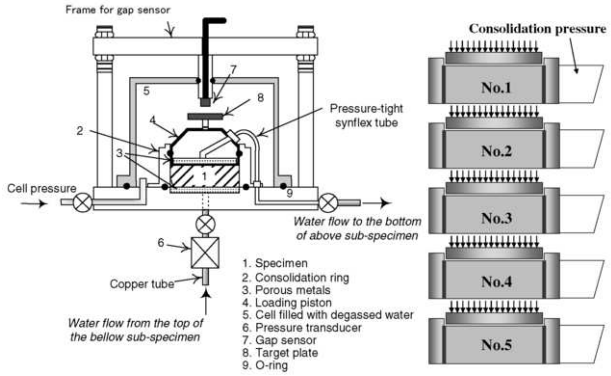

Fig. 2. Schematic layout of the inter-connected consolidation apparatus and illustration of the friction effect.

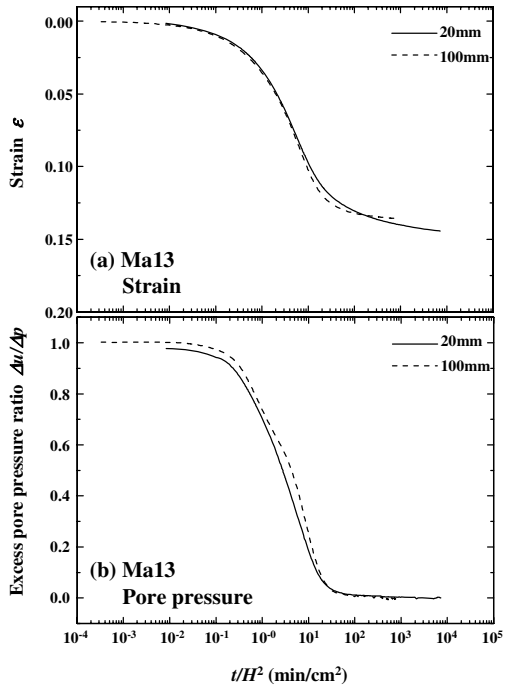

Fig. 3. Temporal variations in the (a) compressive strain defined for the total thickness and (b) excess pore pressure measured at the undrained boundary for Ma13.

and a height of 10 mm (or 20 mm). The equipment is illustrated in Fig.2.

Each consolidometer was filled with deaired water and a backpressure of 98 or 196 kPa was applied. The top piston of a consolidometer and the bottom base metal of one of the other consolidometers were connected by a copper tube through a porous metal disk with a diameter of 55 mm. The drainage copper tubes for all the consolidometers were connected in series. The drainage system had a bypass to switch the connection to pallalel by valve operation. On each base drainage, a pore water pressure transducer was installed. The consolidation pressure was applied into the pressure cell above the loading piston with an o-ring.

In the preliminary consolidation stages, the consolidation pressure was incrementally loaded up to the overburden effective stress σ'_{v0}. In this stage, the drainages were switched to bypass in parallel connection to create the double drainage boundary for all the specimen elements. This condition was maintained for 24 h; then, the drainage was switched to series by valve operation, and the consolidation pressure was increased to a target pressure ($2p_c$). Settlement and pore-water pressure were measured for each specimen element. The settlement was measured by a gap sensor installed at the top of the consolidometer.

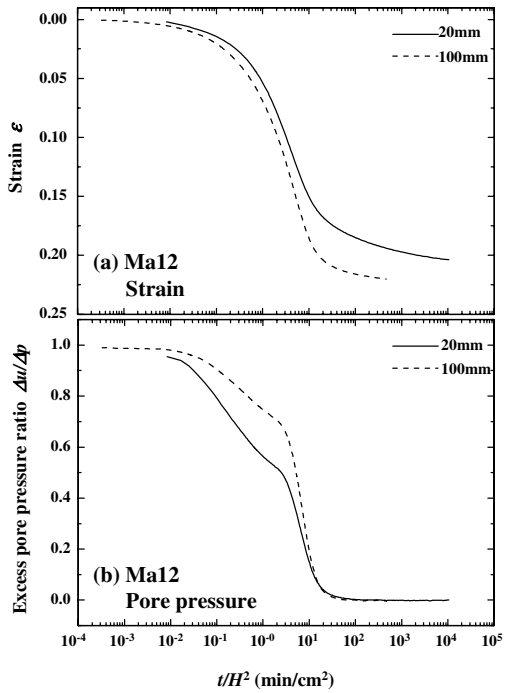

Fig. 4. Temporal variations in the (a) compressive strain defined for the total thickness and (b) excess pore pressure measured at the undrained boundary for Ma12.

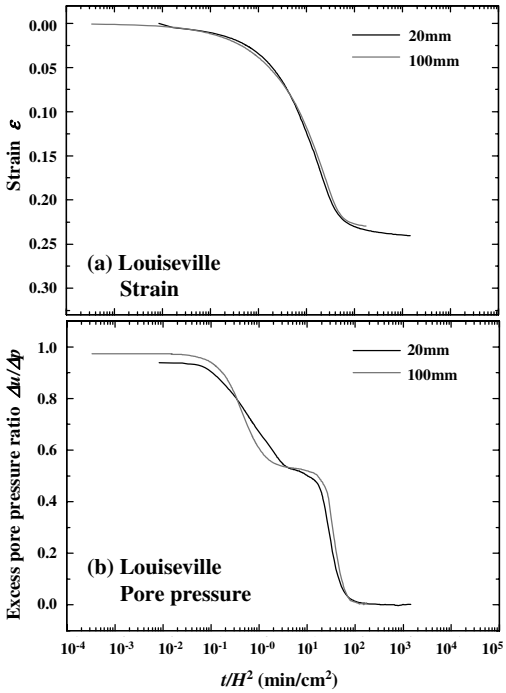

Fig. 5. Temporal variations in the (a) compressive strain defined for the total thickness and (b) excess pore pressure measured at the undrained boundary for Louiseville clay.

3 RESULTS AND DISCUSSIONS

The temporal variations in the (a) compressive strain defined for the total thickness (not for the thickness of each specimen element) and (b) excess pore water pressure measured at the undrained boundary (at the larger specimen number) are shown in Figs.3–5. For each sample, test results with different thicknesses were superimposed. Here, the elapsed time t was divided by the squared maximum drainage distance H, i.e., t/H^2,

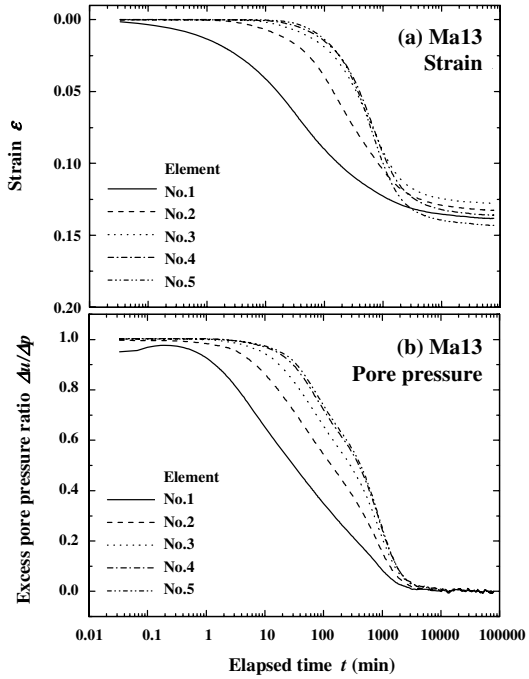

Fig. 6. Temporal variations in the (a) compressive strain and (b) excess pore pressure in each specimen element for Ma13.

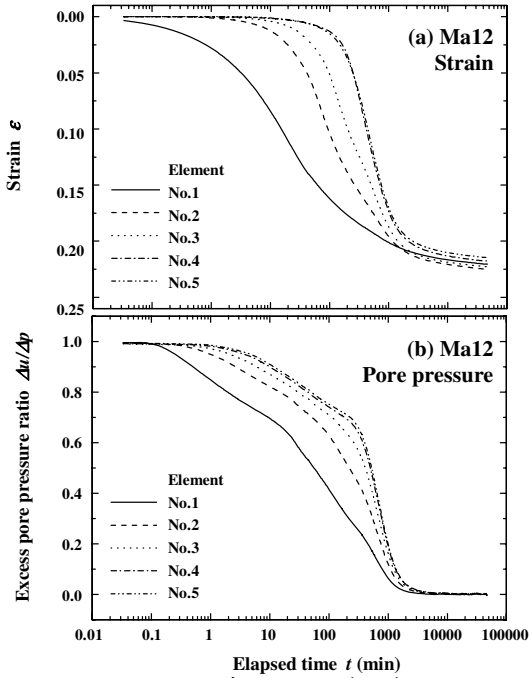

Fig. 7. Temporal variations in the (a) compressive strain and (b) excess pore pressure in each specimen element for Ma12.

where H was defined as the thickness just before the long-term loading. This is equivalent to time factor T_v divided by the coefficient of consolidation c_v, i.e. T_v/c_v.

At the excess pore water pressures, the results for different thicknesses agreed well against t/H^2, indicating that the time corresponding to the EOP was consistent with the law of squared H. In Ma13, the excess pore water pressures and the compressive strains observed in the primary consolidation stage for different thicknesses were equivalent, indicating that the law of squared H was perfectly satisfied. The behavior was classified into hypothesis A, as shown in Fig.1. On the other hand, in Ma12, some significant differences at different thicknesses were seen in the strains, and this fact was close to the hypothesis B. From these tendencies, we can understand that the strain behavior following hypothesis B appeared when the clay sample had a developed structure. However, Louiseville clay with a highly developed structure clearly followed the hypothesis A. Consequently, we can understand that the strain behavior following hypothesis B appeared when the clay sample had structural viscosity, because Ma12 showed significant secondary consolidation (Watabe et al., 2008). The unusual behavior of the excess pore water pressure for Ma12 and Louiseville clays will be described later.

The temporal variations in the (a) compressive strain and (b) excess pore water pressure in each specimen element are shown in Figs.6–8. The excess pore pressure dissipation and increase in consolidation strain were more rapid at a specimen element closer to the drainage (element No.1 was the closest to the drainage). The times when the excess pore water pressures completely dissipated were the same for all the specimen elements in each test. It can be explained that the drained water from the upstream specimen element flowed into the downstream specimen element. From this point of view, the EOP was clearly identified in the excess pore water pressure dissipation rather than in the compressive strain for all the tests. Focusing on the strain behavior of each specimen element, the strain in an element closer to the drainage boundary, particularly specimen element number "1," shows an unclear EOP.

The excess pore pressure dissipations of all the specimen elements were in the order of the distance from the drainage boundary; however, strains were not necessarily in the same order. As mentioned above, the excess pore pressures were in good order caused by the inflow from the upstream specimen

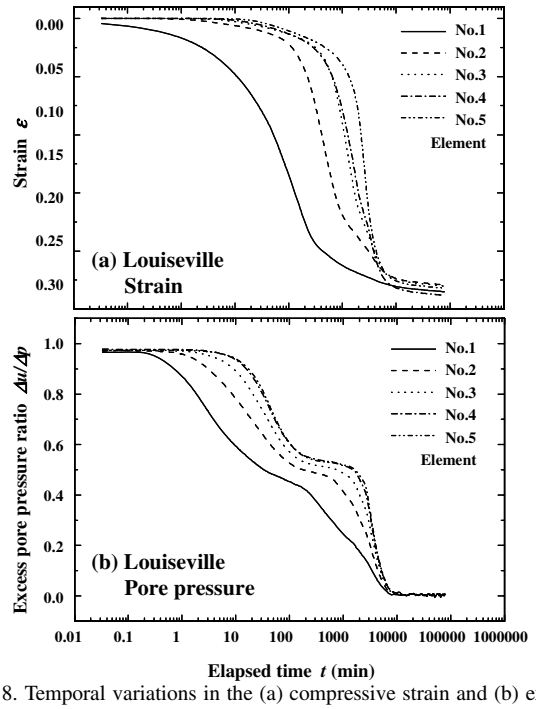

Fig. 8. Temporal variations in the (a) compressive strain and (b) excess pore pressure in each specimen element for Louiseville clay.

element, even if the specimen elements were not perfectly homogeneous. Because the strain was strongly influenced by small differences in the soil properties, the strains were not always in a good order for natural clay deposits, which generally had variable properties.

In Ma12 and Louiseville clays, the temporal variations in the compressive strain followed a normal pattern; however, the excess pore pressure dissipation curves were characterized by an unusual pattern consisting of 2 stages. In Ma12 and Louiseville clays, the excess pore pressure ratio $\Delta u/\Delta p$ suddenly decreased to around 0.7 and 0.5, respectively, at the beginning of the consolidation process and then decreased to zero in the usual manner. The effective stresses at $\Delta u/\Delta p$=0.7 and 0.5 in

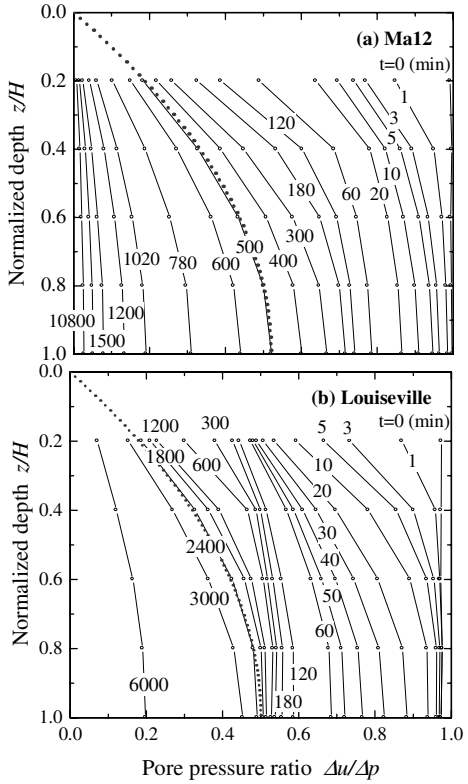

Fig. 9. Isochrones on pore pressure ratio: (a) Ma12 and (b) Louiseville clays.

Ma12 and Louiseville clays, respectively, correspond to the consolidation yield stress in these loading conditions.

The isochrones on excess pore pressure for Ma12 and Louiseville clays are shown in Fig.9. In Ma12, the dissipation rapidly proceeded from the drainage boundary at the beginning, and then the isochrones became to be expressed as a parabolic curve after approximately 500 min. This fact indicates that the dissipation after consolidation yielding is a normal behavior to which Terzaghi's consolidation theory is applicable. In Louiseville clay, the dissipation rapidly proceeded from the drainage boundary at the beginning and settles a relatively uniform depth profile at 180 min, and then the dissipation rapidly proceeded again from the drainage boundary and the isochrones became to be expressed as a parabolic curve after approximately 2400 min.

Tanaka (2005) pointed out the existence of small burrows that serve as vertical drains. The pore pressure decreases suddenly once; after the burrows collapse, the pore-water pressure increases substantially. However, by performing a visual examination and a pore pressure sensitivity examination, we confirmed that the samples tested in this study had no burrows when the backpressure was applied to the specimen. Therefore, there were other causes of the characterized pore pressure dissipation pattern.

Noda et al. (2005) applied Super/subloading Yield Surface Cam-clay model (Asaoka et al., 2002) to a road embankment and explained the observed delayed consolidation as the structural degradation which rises excess pore pressure. The two staged excess pore pressure dissipation observed in this study is similar to this behavior. However, because any pore pressure rise was not observed and strains were monotonically increased throughout the test, we could not confirm the evidence on the structural degradation.

As above mentioned, the temporary stagnation of excess pore pressure dissipation was observed when the effective stress increased to the consolidation yield stress. This indicates that the first and second stages corresponded to the overconsolidation and normal consolidation, respectively. Leroueil et al. (1980) obtained a similar and clearer pore pressure dissipation pattern for sensitive eastern Canada clay with a significantly developed structure. In their explanation for this behavior, the sudden dissipation at the beginning corresponded to a larger coefficient of consolidation in the overconsolidation range and the consequent slow dissipation corresponded to a smaller coefficient of consolidation in the normal consolidation range. Because Ma12 and Louiseville clays had a high water content with a higher developed structure, the explanation of the behavior can be the same as that of Leroueil et al. (1980).

4 CONCLUSIONS

The knowledge newly obtained from this study can be summarized as follows:

1) The law of squared H is essentially valid for the pore water pressure dissipation in specimens with various thicknesses.
2) In Ma13 and Louiseville clays, the strain variation follows hypothesis A. However, in Ma12, the strain variation follows hypothesis B. These facts indicated that the strain behavior following hypothesis B appeared when the clay sample had structural viscosity.
3) In Ma12 and Louiseville clays, the excess pore pressure dissipation curves are characterized by an unusual pattern with two stages. The excess pore pressure ratio $\Delta u/\Delta p$ suddenly decreases to 0.7 and 0.5, respectively, at the beginning of the consolidation process and then decreases to zero as a usual manner.
4) Because Ma12 and Louiseville clays have a high water content with a highly developed structure, the sudden dissipation at the beginning corresponds to a larger coefficient of consolidation in the overconsolidation range and the consequent slow dissipation corresponds to a smaller coefficient of consolidation in the normal consolidation range.

ACKNOWLEDGEMENTS

The study presented in this paper was carried out as a part of the collaborative research between Port and Airport Research Institute and Kansai International Airport Land Development Co., Ltd.

REFERENCES

Aboshi, H. 1973. An experimental investigation on the similitude in the consolidation of a soft clay, including the secondary creep settlement. *Proc. 8th Int. Conf. Soil Mech. Found. Engg.,* Moscow, Vol. 4(3): p88.

Asaoka, A., Noda, T., Yamada, T., Kaneda, K. and Nakano, M. 2002. An elasto-plastic description of two distinct volume change mechanisms of soils, *Soils and Foundations*, 42(5), 47–57.

Jamiolkowski, M., Ladd, C.C., Germaine, J.T. and Lancellotta, R. 1985. New developments in field and laboratory testing of soils. *Proc.11th Int. Conf. Soil Mech. Found. Engg.*, San Francisco, Vol. 1, 57–153.

Ladd, C.C., Foott, R., Ishihara, K., Schlosser, F. and Poulos, H.G. 1977. Stress-deformation and strength characteristics. State-of-the-Art Report, *Proc. 9th Int. Conf. Soil Mech. Found. Engg.*, Tokyo, Vol. 2, 421–494.

Leroueil, S., Le Bihan, J.P. and Tavenas, F. 1980. An approach for the determination of the preconsolidation pressure in sensitive clays, *Can. Geotech. J.* 17(3), 446–453.

Noda, T., Asaoka, A. Nakano, M., Yamada, E. and Tashiro, M. 2005. Progressive consolidation settlement of naturally deposited clayey soil under embankment loading, *Soils and Foundations*, 45(5), 39–51.

Tanaka, H. 2005. Consolidation behavior of natural soils around p_c value—Inter-connected oedometer test, *Soils and Foundations*, 45(3), 97–105.

Watabe, Y., Udaka, K. and Morikawa, Y. 2008. Strain rate effect on long-term consolidation of Osaka bay clay, *Soils and Foundations*, 48(4), 495–509.